

Onset of the Somali Jet in the Arabian Sea During June 1997

David Halpern

and

Peter M. Woiceshyn

Earth and Space Sciences Division

Jet Propulsion Laboratory

California Institute of Technology

Pasadena, CA 91109

**Abstract.** The National Aeronautics and Space Administration scatterometer (NSCAT) surface wind vectors are used to describe the rapid onset of the Somali Jet throughout the Arabian Sea. In June 1997 the time of Somali Jet onset varied over the Arabian Sea, with 17 - 18 June the average time. The Somali Jet appeared first in the western Arabian Sea, expanded over two weeks to encompass the Arabian Sea, and produced a 3-fold increase in surface wind convergence in the eastern Arabian Sea. The onset time of the  $12 \text{ m s}^{-1}$  isotach preceded by 3 - 4 days the onset of monsoon rainfall in Goa. For Somali Jet wind speeds above  $10 \text{ m s}^{-1}$ , the 2-day  $1^\circ \times 1^\circ$  sea surface temperature decreased  $0.5^\circ\text{C}$  per  $1 \text{ m s}^{-1}$  increase in colocated wind speed. The Somali Jet created a north-south distribution of Ekman pumping and suction in the central Arabian Sea to enhance the eastward surface current by  $0.1 \text{ m s}^{-1}$ . The Somali Jet doubled the southward Ekman transport across the southern boundary of the Arabian Sea. In June 1997 when the most-intense El Niño episode of the century was in its onset phase, the southward Ekman transport across the southern boundary of the Arabian Sea was one-half that observed since 1992.

## 1. Introduction

The onset of the Somali Jet, which is the intense southwesterly surface wind over the Arabian Sea during the summer monsoon, is believed to precede the onset of rainfall along the west coast of India [Desai *et al.*, 1976; Krishnamurti *et al.*, 1981; Yadav and Kelkar, 1989]. Near Somalia the onset duration is about one week [Fieux and Stommel, 1977]. Until June 1997 when satellite-borne instrumentation measured surface wind vectors with adequate sampling, there were insufficient surface wind vector data to describe the rapid onset throughout the Arabian Sea.

A 2-day  $1^\circ$ -latitude  $\times$   $1^\circ$ -longitude surface wind vector data product was created from National Aeronautics and Space Administration (NASA) scatterometer (NSCAT) measurements of surface roughness [Graf *et al.*, 1998]. NSCAT data are used to describe Arabian Sea winds during June 1997. Every 2 days NSCAT recorded 20 - 40 instantaneous 25-km  $\times$  25-km wind velocities in nearly every  $1^\circ \times 1^\circ$  area. The root-mean-square (rms) accuracy of NSCAT 10-m

1 height wind speed was  $1 \text{ m s}^{-1}$  [Freilich and Dunbar, 1999]. The last day of data was 29 June  
2 1997 because of an accident to the satellite solar panels.

3 Prior to the NSCAT launch in August 1996, surface wind vector data products consisted of  
4 ship reports, data-assimilation forecast-analysis simulations made at a numerical weather prediction  
5 (NWP) center, European Remote Sensing (ERS) satellite scatterometer wind vector measurements,  
6 and their combination. Ship-wind observations are too sparse to delineate the Somali Jet onset  
7 over the Arabian Sea, e. g., during June 1997 only 15% of the  $1^\circ \times 1^\circ$  areas had at least one ship  
8 report every 2 days. Because of data-assimilation procedures NWP wind vector products do not  
9 adequately capture horizontal scales of motion for distance less than about 500 km [Halpern *et al.*,  
10 1999], which would alias the narrowness of the Somali Jet. The ERS orbit and one-sided (in  
11 contrast to the two-sided NSCAT) scatterometer yielded data with a minimum 3-day repeat cycle,  
12 which would alias the rapid Somali Jet onset.

13 Our NSCAT findings include the first description of the Somali Jet as it developed across the  
14 Arabian Sea. The Somali Jet produces a unique climatological feature: sea surface temperature is  
15 lower in July than in April [Hastenrath and Lamb, 1979]. We present an empirical relationship  
16 between the increase of NSCAT wind speed and the decrease of satellite-derived sea surface  
17 temperature at 2-day intervals; previous studies considered time intervals of 1 month, which could  
18 not be representative of wind-mixing processes in the Arabian Sea where the 2- to 3-day inertial  
19 period is the appropriate time scale. The asymmetrical distribution of phytoplankton north and south  
20 of the axis of the Somali Jet is believed to be caused by the wind-forced vertical velocity at the  
21 bottom of the Ekman layer [Brock *et al.*, 1991], named  $w_E$ . We show the rapid evolution of  $w_E$ ,  
22 which heretofore had not been documented. An explanation for the time difference between the  
23 times of onset of the Somali Jet in the western Arabian Sea and rainfall along the central part of the  
24 west coast of India is explored with NSCAT-derived surface wind convergence and satellite-  
25 derived integrated cloud liquid water content. Sea surface temperature and integrated cloud liquid  
26 water content data were measured from Advanced Very-High Resolution Radiometer (AVHRR)  
27 and Special Sensor Microwave Imager (SSM/I) instruments, respectively.

## 2. Somali Jet

There is no definition for the onset of the Somali Jet. Appropriate characteristics for the onset of the Somali Jet are wind direction towards India, sustained wind speeds above  $7.5 \text{ m s}^{-1}$ , May or June for the time of occurrence, and the rise in wind speed would occur over about 1 week. The  $7.5 \text{ m s}^{-1}$  threshold, which corresponds to the approximate average wind speed over the global ocean, is chosen because Somali Jet speeds would be greater than the global average wind speed. During June - August the largest surface wind speeds in the Northern Hemisphere are found in the Arabian Sea [*da Silva et al.*, 1997]. Conditions of southwesterly direction and speed greater than  $7.5 \text{ m s}^{-1}$  must persist for at least six consecutive days, which is 2 - 3 inertial periods in the Arabian Sea and is the time associated with development of Ekman currents. With this definition, the average start time of the Somali Jet over the Arabian Sea was 17 - 18 June 1997.

The onset time was not the same throughout the Arabian Sea (Figure 1). Sixteen percent of the Arabian Sea ( $8^{\circ}\text{N} - 24^{\circ}\text{N}$ ,  $50^{\circ}\text{E} - 77^{\circ}\text{E}$ ) had a single onset time of 15 - 16 June and in another 16% the onset time was 17 - 18 June, with nearly all these areas occurring between  $60^{\circ}\text{E}$  and  $70^{\circ}\text{E}$ . West of  $60^{\circ}\text{E}$  and north of  $20^{\circ}\text{N}$ , many  $1^{\circ} \times 1^{\circ}$  regions had multiple onset times, with the first onset in May, which is the time portrayed in Figure 1. Where multiple onsets occurred, wind speeds subsequently dropped below  $7.5 \text{ m s}^{-1}$  and then in mid-June the wind speed increased above  $7.5 \text{ m s}^{-1}$ , which was maintained until the end of the record on 29 June.

High winds were defined to be above  $12 \text{ m s}^{-1}$ , which produce rough seas. At the time of the Somali Jet onset, high wind speeds did not occur simultaneously throughout the Arabian Sea. The  $12 \text{ m s}^{-1}$  isotach first appeared on 15 - 16 June in a small area off Somalia, but not adjacent to the coast (Figure 2), indicating acceleration of the Somali Jet as it penetrated the Arabian Sea. Coastal upwelling lowered sea surface temperature which lowered air temperature over the coastal ocean to produce a southwesterly geostrophic wind offshore of Somalia to locally enhance the Somali Jet. As the Somali Jet marched across the Arabian Sea, the cross-stream dimension expanded. On 29 June when high wind speeds were first observed along  $70^{\circ}\text{E}$ , the Somali Jet engulfed nearly the

entire Arabian Sea. During the initial two weeks after the onset of monsoon winds, the easternmost extent of the  $12 \text{ m s}^{-1}$  isotach moved 1000 km eastward at about  $1 \text{ m s}^{-1}$ .

Very high wind speeds, which were those above  $15 \text{ m s}^{-1}$  and which a seaman would characterize to be a moderate gale, appeared intermittently. The  $15 \text{ m s}^{-1}$  isotach first appeared on 19 - 20 June when it was centered at  $15^{\circ}\text{N}$ ,  $59^{\circ}\text{E}$  (Figure 2). It next appeared on 27 - 28 June, and the following day the  $15 \text{ m s}^{-1}$  isotach covered a greatly expanded region centered at  $14^{\circ}\text{N}$ ,  $61^{\circ}\text{E}$ . On 29 June, an additional patch of gale winds was located near Somalia. Perhaps the secondary patch off Somalia represented the beginning of the second active monsoon interval, analogous to active and lull rainfall periods over India.

Two features associated with monsoon winds were not observed. An onset vortex has occurred over the Arabian Sea on 37 occasions during 1901 - 1968 [Krishnamurti *et al.*, 1981], but was not observed in June 1997 (Figure 2). The two-branch structure of the Findlater Jet [Findlater, 1969], which is the intense southwesterly wind at 1-km height, was not observed (Figure 2). A split Somali Jet was also not observed in July 1995 [Halpern *et al.*, 1998].

### 3. Time Interval Between Onsets of Somali Jet and Rainfall

The onset of monsoon rainfall along the west coast of India begins in the south, usually in early June, and moves northward, reaching Mumbai (Bombay) about 10 - 15 days later [Dhar *et al.*, 1980]. The India Meteorological Department definition of onset time of monsoon rainfall involves observations from more than a single site and a threshold rainfall amount dependent upon locality. We chose Goa, a small coastal state at about  $15^{\circ}\text{N}$ , where India's National Institute of Oceanography is located. The time of monsoon rainfall onset is the second day in a series of at least three consecutive days in which each daily rainfall accumulation is 5 cm or more. Ample rainfall for three successive days delineates the approximate 1-week interval of pre-monsoon showers, which sometimes are quite intense but which would not yield substantial rainfall for 3 successive days. The arbitrarily-defined 5-cm threshold value was 5-fold the daily amount measured during June - September 1997 [Bell and Halpert, 1998]. For June 1997, daily rainfalls

1 at four stations (Vengurla, Dabolim, Mormugao, Panjim) were averaged, and the onset time of  
2 monsoon rainfall at about 15°N was 19 June (Figure 3), which was about 12 days after the usual  
3 time of occurrence [Dhar *et al.*, 1980]. June 19 was 3 - 4 days after the appearance of the 12 m s<sup>-1</sup>  
4 isotach in the Arabian Sea. The rainfall onset phase lasted about a week. In June 1997, the first  
5 lull lasted 6 days, which is typical. The next active phase began with a deluge on 29 June (Figure  
6 3), when the Somali Jet reached 70°E and covered most of the Arabian Sea.

7 We hypothesize that the time interval between the onsets of the Somali Jet in the western  
8 Arabian Sea and rainfall in Goa is related to wind divergence. Horizontal wind divergence (or  
9 convergence, which is equal to the negative value of divergence) was computed with the 1° x 1°  
10 time-averaged east-west and north-south wind components for 4 - 16 and 17 - 29 June (Figure 4).  
11 Before onset of the Somali Jet, the surface wind was divergent (convergent) west (east) of 60°E  
12 and the trend of the zero-divergence isoline near 60°E was approximately northeast-southwest.  
13 During 4 - 16 June, the average convergence east of 60°E was  $0.8 \times 10^{-6} \text{ s}^{-1}$ . After onset of the  
14 Somali Jet, the zero-divergence isoline near 60°E became aligned approximately parallel to the west  
15 coast of India. During 17 - 29 June, the average convergence east of 60°E was  $2.8 \times 10^{-6} \text{ s}^{-1}$ , more  
16 than a 3-fold increase. Horizontal gradient computational noise and aliasing of small-scale wind  
17 fluctuations stymied estimation of surface wind convergence at 2-day intervals, making it very  
18 difficult to determine with NSCAT data whether surface wind convergence in the eastern Arabian  
19 Sea had intensified before the onset of monsoon rainfall in Goa.

20 Integrated water vapor (also called total precipitable water) and integrated cloud liquid water  
21 content data produced by Ferraro *et al.* [1996] are used to show the reasonableness of a linkage  
22 between increased surface wind convergence and rainfall. During northern hemisphere summer,  
23 the moistest air throughout the global atmosphere is over the Indian Ocean, where the integrated  
24 water vapor is nearly 60 mm [Ferraro *et al.*, 1996]. Over the eastern Arabian Sea, the average  
25 amount of integrated water vapor during 4 - 16 June and 17 - 29 June 1997 differed by 2%, which  
26 is one-fifth of the 10% uncertainty associated with an estimate of integrated water vapor. Thus, the  
27 moistness of the air was the same before and after the onset of the Somali Jet. In contrast, the

1 integrated cloud liquid water content east of 60°E was 40% larger during 17 - 29 June compared to  
2 4 - 16 June 1997. The increase in integrated cloud liquid water was more than 2-fold greater than  
3 the expected error [Weng *et al.*, 1997]. It is tempting to speculate that the increased surface wind  
4 convergence created by the Somali Jet as it marched across the Arabian Sea pumped moist air  
5 upwards where condensation occurred. Intense evaporation would presumably supply enough  
6 water vapor for the air to remain saturated.

#### 8 **4. Wind-Driven Ocean-Atmosphere Interactions**

##### 9 **4.1 Sea Surface Temperature**

10 After the onset of the Somali Jet, sea surface temperature lowering in the Arabian Sea is  
11 influenced by upwelling and entrainment of colder water from below, offshore advection of colder  
12 water from coastal upwelling areas, evaporation, and solar radiation. We describe the total change  
13 in sea surface temperature following the development of the Somali Jet; it is beyond the scope of  
14 this study to describe the relative importance of different processes affecting sea surface  
15 temperature. Clouds prevented 2-day 1° x 1° AVHRR data from having the excellent coverage of  
16 NSCAT, which operated at cloud-piercing microwave frequencies. Sea surface temperatures  
17 averaged over 1 - 14 June represented the pre-monsoon sea surface temperature field. Beginning  
18 15 - 16 June the 2-day 1° x 1° AVHRR sea surface temperature difference from the pre-monsoon  
19 value were collocated with NSCAT wind speed. On 15 - 16 June and 17 - 18 June, when no  
20 AVHRR sea surface temperature retrievals had occurred in the high wind speed area near Somalia,  
21 the collocated wind speeds were low, solar radiative heating of the ocean continued, and the  
22 average collocated sea surface temperature rose 0.2°C (Figure 5), which was less than the 0.5°C  
23 rms accuracy of global AVHRR data for June 1997 [Halpern *et al.*, in preparation]. AVHRR and  
24 NSCAT matchups in the high wind speed region first occurred on 19 - 20 June when the average  
25 collocated sea surface temperature dropped 1.0°C and the average collocated wind speed was 9.6 m  
26 s<sup>-1</sup>. During 23 - 29 June, the average collocated sea surface temperature decreased almost linearly  
27 with wind speed, i. e.,  $\Delta\text{SST} (^{\circ}\text{C}) = -0.6 S (\text{m s}^{-1}) + 5.3$ , where  $\Delta\text{SST}$  is the 2-day 1° x 1° average

1 sea surface temperature difference relative to the pre-monsoon onset and S, collocated wind speed,  
2 was between 10.5 and 12.5 m s<sup>-1</sup>.

#### 4 4.2 Ekman Transport

5 Employing conservation of mass, a lowest-order approximation of southwest monsoon  
6 ocean circulation in the Arabian Sea is southward flow across the southern boundary along 8.5°N,  
7 flow from the thermocline into the near-surface layer, and water entering the Arabian Sea by the  
8 western boundary Somali Current. Attention is focused on the southward Ekman transport along  
9 8.5°N because it is an important feature in the meridional overturning of the Indian Ocean. Also, it  
10 was a subject of a recent oceanographic expedition [*Chereskin et al.*, 1997]. The method to  
11 compute southward Ekman transport is described by *Halpern et al.* [1998]; however, herein wind  
12 stresses were computed from the Cartesian components of each wind vector.

13 During 4 - 16 June (before onset of Somali Jet) and 17 - 29 June (after onset of Somali Jet),  
14 the southward Ekman transports along the southern boundary of the Arabian Sea at 8.5°N were 4.4  
15 and  $9.9 \times 10^6 \text{ m}^3 \text{ s}^{-1}$  ( $1 \times 10^6 \text{ m}^3 \text{ s}^{-1} = 1 \text{ Sv}$ ), respectively, i. e., the Somali Jet doubled the southward  
16 Ekman transport at 8.5°N. A 3-Sv Ekman transport along the southern boundary of the Arabian  
17 Sea is a criterion for significant difference because it would correspond to an Ekman current  
18 averaged over a 50-m thick layer of 2 cm s<sup>-1</sup>, which is a measurable quantity.

19 June 1997 was coincident with the onset phase of the most intense El Niño in a hundred  
20 years. Whether the June 1997 surface winds over the Arabian Sea had been influenced by El Niño  
21 is explored with the southward Ekman transport at 8.5°N. A priori we did not anticipate the El  
22 Niño to exert a strong effect because the correlation coefficient between the Indian monsoon and El  
23 Niño was 0.5 [*Webster et al.*, 1998], indicating only 25% of the variances were linearly related.  
24 Allowing the 1 - 29 June interval to represent the entire month, the June monthly mean NSCAT  
25 southward Ekman transport across the southern boundary of the Arabian Sea was 7.3 Sv, which  
26 was nearly identical to that (7.6 Sv) computed with ERS scatterometer data. Using ERS wind  
27 vector measurements, the June 1992, 1993, 1994, and 1995 monthly mean southward Ekman



transports were 13.4, 13.0, 15.1, and 13.5 Sv, respectively [Halpern *et al.*, 1998]; for June 1996 and 1998 the results were 14.6 and 13.6 Sv, respectively. The mean southward Ekman transport for June 1992 - 1996 and 1998 was 13.9 Sv. The interannual range was less than 3 Sv and, therefore, not significant. Thus, the June 1997 southward Ekman transport at 8.5°N was about 6.6 Sv (or 50%) lower than that found for six other years. Inspection of June charts of June mean wind speed and direction showed that the Somali Jet along 8.5°N in June 1997 was 1 - 2 m s<sup>-1</sup> slower in the western and eastern Arabian Sea and the direction in the eastern Arabian Sea had a stronger southerly component compared to June of the other years. The cause of the anomalous zonal wind stresses along 8.5°N in June 1997 is unknown, although it is tempting to speculate that it was related to the 1997 El Niño episode.

#### 4.3 Ekman Pumping and Suction

Ekman pumping and suction are the downward and upward, respectively, vertical velocities at the bottom of the Ekman layer. The method to compute  $w_E$  from wind stress components is described by Halpern *et al.* [1998]. During 4 - 16 June,  $w_E$  had relatively small speeds and did not display the north-south pattern of upward and downward motions (Figure 6) associated with monthly mean monsoon winds. During 17 - 29 June, upwelling (downwelling) occurred north (south) of the approximate position of the axis of the Somali Jet (Figure 6). The  $w_E = 0$  isoline had a quasi-zonal distribution across the Arabian Sea by 19 - 20 June 1997, indicating a local set-up time for Ekman pumping and suction of about 2 - 3 inertial periods after onset of the Somali Jet.

An oceanographic tenet is that fluctuations of  $w_E$  and thermocline depth are inversely related; therefore, an eastward ocean current should develop in the central Arabian Sea in response to the Somali Jet. Variations of thermocline depth are represented by satellite-derived sea surface height data recorded by the Ocean Topography Experiment satellite, named TOPEX/Poseidon. Attention is focused on the 60 - 65°E zone north and south of about 15°N where the  $w_E = 0$  isotach was nearly zonal after the Somali Jet onset. The average 60°E - 65°E July-minus-May 1997 sea surface height at 14.5°N was 19 cm higher than that at 18.5°N, with an approximate linear slope between

1 14.5°N and 18.5°N. The  $4.2 \times 10^{-7}$  north-south sea surface slope corresponds to  $0.1 \text{ m s}^{-1}$  eastward  
2 surface geostrophic current in July relative to that in May. This was equal to the average eastward  
3 motion of 15-m drogued satellite-tracked drifters (serial numbers 19163, 19168 and 19830 in May  
4 and July, 19834 in May, 19829 in July) located from 13°N to 20°N.

5 In June 1997 the value of  $w_E$  integrated over the Arabian Sea, was  $-2.4 \text{ Sv}$ , i. e., the vertical  
6 transport of water was from the Ekman layer into the thermocline. The June 1997 direction of the  
7 vertical transport was opposite to that determined for June 1992 - 1995 [Halpern *et al.*, 1998] and  
8 1996 and 1998. In June 1992 - 1996 and 1998 the mean  $\pm$  standard deviation and minimum value  
9 of the vertical transports were  $5.7 \pm 1.3$  and  $3.5 \text{ Sv}$ , respectively. The vertical transport difference  
10 between the June 1997 value and the minimum value for six other years was, when converted to  
11 vertical velocity, nearly three times larger than the  $0.6 \times 10^{-6} \text{ m s}^{-1}$  uncertainty associated with  
12 vertical velocity estimated from the continuity equation and horizontal current measurements.

## 14 5. Discussion

15 The high-sampling attribute of NSCAT has been used to describe the onset of the Somali Jet  
16 and associated ocean-atmosphere interactions in the Arabian Sea in June 1997. The 3- to 4-day  
17 earlier time of onset of the  $12 \text{ m s}^{-1}$  isotach compared to the time of onset of monsoon rainfall in  
18 Goa was related to the movement of the Somali Jet across the Arabian Sea and the associated  
19 development of a 3-fold increase in surface wind convergence. We suggest that deceleration of the  
20 Somali Jet by the Indian subcontinent produced intense surface wind convergence in the eastern  
21 Arabian Sea; this hypothesis should be tested with atmospheric model simulations made with and  
22 without mountains. A consequence of the Somali Jet slowing down would be an increase in  
23 upward flux of moisture, which was represented by a 40% rise in total amount of cloud liquid  
24 water in the eastern Arabian Sea. Orographic uplift also contributed towards rainfall formation.  
25 The Somali Jet lowered sea surface temperature of about  $0.5^\circ\text{C}$  per  $1 \text{ m s}^{-1}$  increase in wind speed  
26 for wind speeds from  $10 - 13 \text{ m s}^{-1}$ ; however, the sea surface temperature remained above  $27^\circ\text{C}$  so  
27 that the tendency for atmospheric convection was high. The Somali Jet introduced a meridional

1 distribution of  $w_E$  in the central Arabian Sea, which could have created a north-south tilt of sea  
2 level to enhance the eastward geostrophic current by  $0.1 \text{ m s}^{-1}$  in July compared to May; this is  
3 consistent with climatology [Molinari *et al.*, 1990; Hastenrath and Greischer, 1991].

4 In June 1997, the time of onset of monsoon rainfall in Goa was 12-days later than normal,  
5 the southward Ekman transport at  $8.5^\circ\text{N}$  was 50% of normal, and the vertical transport was  
6 downward from the Ekman layer instead of upward into the Ekman layer. It is possible that the  
7 onset of the 1997 El Niño episode affected the early phase of the Indian monsoon, which would be  
8 difficult to demonstrate because of the multiplicity of factors that produce the monsoon. The  
9 anomalies did not influence the June - September strength of All-India rainfall, which was normal.

10 Although NSCAT provided surface wind vectors with high accuracy and unprecedented  
11 sampling in time and space, a recommendation is made for a data product of similar accuracy and  
12 higher sampling. Additional wind observations are required each day to reduce the uncertainty of  
13 the onset time of the Somali Jet to 1 day, which would increase the effectiveness of the rainfall  
14 forecast. Higher temporal sampling would reduce computational noise of horizontal gradients  
15 associated with surface wind convergence. Surface wind convergence at 1-day intervals is  
16 necessary to develop an empirical relationship between intensity of convergence and rainfall for  
17 active and lull monsoon periods. Wind vectors recorded more frequently would yield a measure of  
18 diurnal-period wind fluctuation, which influence phytoplankton blooms [McCreary, J. P., Jr.,  
19 personal communication, 1998]. Enhanced sampling of NSCAT-accuracy winds is likely with the  
20 scheduled launches of NASA's QuikScat in 1999 and NASA's SeaWinds in 2000.

21  
22 **Acknowledgements.** We are grateful to the following people who kindly provided data: Dr. R.  
23 Ferraro (National Oceanic and Atmospheric Administration) for SSMI integrated water vapor and  
24 SSMI total liquid water content data; Dr. R. Kelkar (India Meteorological Department) for rainfall  
25 observations; S. Pouliquen (Centre ERS d'Archivage et de Traitement) for ERS wind vectors; Dr.  
26 R. Reynolds (NOAA National Centers for Environmental Prediction) for AVHRR sea surface  
27 temperatures; Dr. R. Molinari (NOAA Atlantic Oceanographic and Meteorological Laboratories)

1 and Dr. D. Olson (University of Miami) for drifter-buoy positions. Dr. S. Hastenrath (University  
2 of Wisconsin) provided valuable comments on an early version of the manuscript. Helpful  
3 comments by two anonymous reviewers greatly clarified the presentation. The research described  
4 in this paper was performed, in part, by the Jet Propulsion Laboratory, California Institute of  
5 Technology, under contract with the National Aeronautics and Space Administration.

## 7 References

8 Bell, G., and M. Halpert, Climate assessment for 1997, *Bull. Amer. Meteor. Soc.*, 79, S1-S50,  
9 1998.

10 Brock, J. C., C. R. McClain, M. E. Luther, and W. W. Hay, The phytoplankton bloom in the  
11 northwestern Arabian Sea during the southwest monsoon of 1979, *J. Geophys. Res.*, 96,  
12 20613-20622, 1991.

13 Chereskin, T. K., W. D. Wilson, H. L. Bryden, A Ffield, and J. Morrison, Observations of the  
14 Ekman balance at 8°30'N in the Arabian Sea during the 1995 southwest monsoon, *Geophys.*  
15 *Res. Lett.*, 24, 2541-2544.

16 Desai, N. N., N. Rangachari, and S. K. Subramanian, Structure of low-level jet-stream over the  
17 Arabian Sea and the Peninsula as revealed by observations in June and July during the monsoon  
18 experiment 1973 and probable origin, *Indian J. Met. Hydro. Geophys.*, 27, 263-274, 1976.

19 Dhar, O. N., P. Rakhecha, and B. Mandal, Does early or late onset of monsoon provide any clue  
20 to subsequent rainfall during the monsoon season?, *Mon. Wea. Rev.*, 108, 1069-1072, 1980.

21 Ferraro, R. R., F. Weng, N. C. Grody, and A. Basist, An eight-year (1987-1994) time series of  
22 rainfall, clouds, water vapor, snow cover, and sea ice derived from SSM/I measurements,  
23 *Bull., Amer. Meteor. Soc.*, 77, 891-905, 1996.

24 Fieux, M., and H. Stommel, Onset of the southwest monsoon over the Arabian Sea from marine  
25 reports of surface winds: Structure and variability, *Mon. Wea. Rev.*, 105, 231-236, 1977.

26 Findlater, J., Mean monthly air flow at low levels over the western Indian Ocean. *Geophys.*  
27 *Mem.*, No. 115, H. M. S. O., London, 53 pp., 1971.

1 Freilich, M. H., and R. S. Dunbar, The accuracy of the NSCAT-1 vector winds: Comparison with  
2 NDBC buoys, *J. Geophys. Res.*, in press, 1999.

3 Graf, J., C. Sasaki, C. Winn, W. T. Liu, W. Tsai, and M. Freilich, NASA scatterometer  
4 experiment, *Asta Astronautica*, 43, 397-407, 1998.

5 Halpern, D., M. H. Freilich, and R. A. Weller, Arabian Sea surface winds and ocean transports  
6 determined from ERS-1 scatterometer, *J. Geophys. Res.*, 103, 7799-7805, 1998.

7 Halpern, D., M. H. Freilich, and R. A. Weller, ECMWF and ERS-1 surface winds over the  
8 Arabian Sea during July 1995, *J. Phys. Oceanogr.*, in press, 1999.

9 Hastenrath, S., and P. J. Lamb, *Climatic Atlas of the Indian Ocean*, vol. 1, *Surface Climate and*  
10 *Atmospheric Circulation*, 116 pp., Univ. Wisconsin Press, Madison, 1979.

11 Hastenrath, S., and L. Greischer, The monsoonal current regimes of the tropical Indian Ocean:  
12 Observed surface flow fields and their geostrophic and wind-driven components, *J. Geophys.*  
13 *Res.*, 96, 126129-12633, 1991.

14 Krishnamurti, T. N., P. Ardanuy, Y. Ramanathan, and R. Pasch, On the onset vortex of the  
15 summer monsoon, *Mon. Wea. Rev.*, 109, 344-363, 1981.

16 Molinari, R., D. Olson, and G. Reverdin, Surface currents in the tropical Indian Ocean derived  
17 from compilations of surface buoy trajectories, *J. Geophys. Res.*, 95, 7217-7238, 1990.

18 da Silva, A. M., C. Young-Molling, and S. Levitus, *Atlas of surface marine 1994*, NOAA Atlas  
19 NESDIS 17, National Oceanic and Atmospheric Administration, Washington, 91 pp, 1997.

20 Webster, P. J., V. O. Magaña, T. N. Palmer, J. Shukla, R. A. Tomas, M. Yanai, and T.  
21 Yasunari, Monsoons: Processes, predictability, and the prospects for prediction, *J. Geophys.*  
22 *Res.*, 103, 14451-14510, 1998.

23 Weng, F., N. C. Grody, R. Ferraro, A. Basist, and D. Forsyth, Cloud liquid water climatology  
24 from the Special Sensor Microwave/Imager, *J. Climate*, 10, 1086-1098, 1997.

25 Yadav, B. R., and R. R. Kelkar, Lower level wind flow over the Indian Ocean during the onset of  
26 monsoon -1987, *Mausam*, 40, 323-328, 1989.

## List of Figures

- 1
- 2 Figure 1. Distribution of times of onset of monsoon wind in  $1^\circ \times 1^\circ$  areas throughout the Arabian
- 3 Sea. No onset time was determined in the white-color areas.
- 4 Figure 2. NSCAT 2-day  $1^\circ \times 1^\circ$  averaged scalar wind speeds for wind speeds  $\geq 12 \text{ m s}^{-1}$  and
- 5 associated vector-averaged directions from 15-16 June to 27-28 June 1997 and 1-day values for 29
- 6 June 1997. Times are shown in upper-left corner of each panel. One-size arrows delineate wind
- 7 direction and are placed at  $2^\circ$  intervals for visual clarity.
- 8 Figure 3. Daily rainfall averaged over four coastal stations near  $15^\circ\text{N}$ . Vengurla is located just
- 9 north of Goa, the other stations are in Goa (Dabolim airport, Panjim harbor, and Panjim city), and
- 10 the distance between Vengurla and Panjim is 25 km. Dotted line represents the 5 cm per day
- 11 threshold rainfall.
- 12 Figure 4. Surface wind divergence (positive values) and convergence (negative values) computed
- 13 from the mean 4 - 16 June and 17 - 29 June 1997 east-west and north-south wind components in
- 14  $1^\circ \times 1^\circ$  areas. Shaded region represents convergence. Contour interval is  $10 \times 10^{-6} \text{ s}^{-1}$ .
- 15 Figure 5. Average collocated values over the Arabian Sea of the difference in sea surface
- 16 temperature between a post-monsoon 2-day mean value and the pre-monsoon mean 1 - 14 June
- 17 1997 sea surface temperature, represented by  $\Delta\text{SST}$ , and the collocated wind speed.
- 18 Figure 6. Vertical velocity at the bottom of the Ekman layer during 4 - 16 June and 17 - 29 June
- 19 1997. Downward motion is shaded. Contour interval is  $10^{-6} \text{ m s}^{-1}$ .

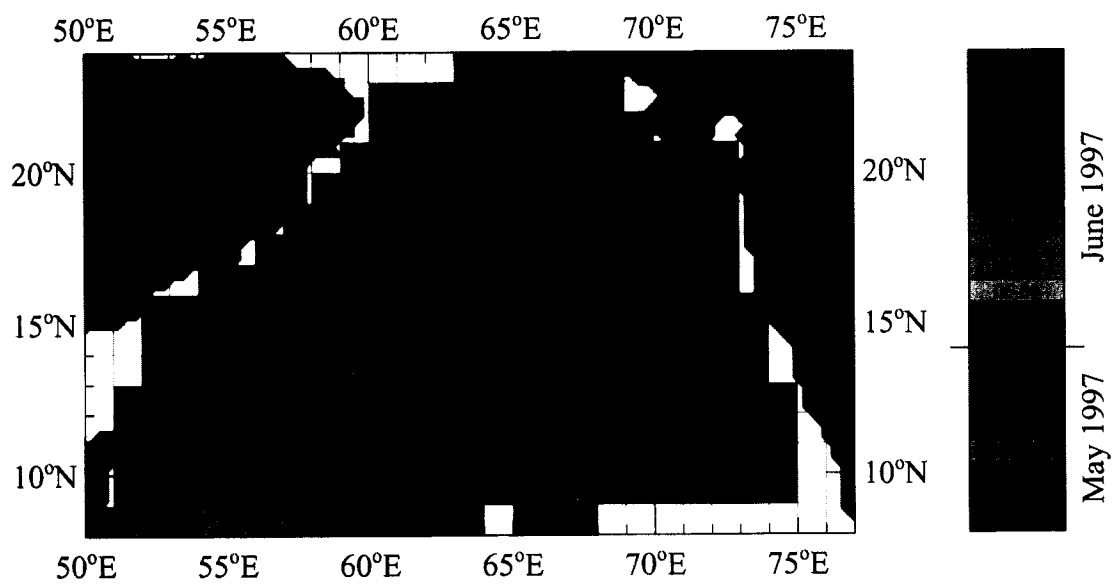


Figure 1

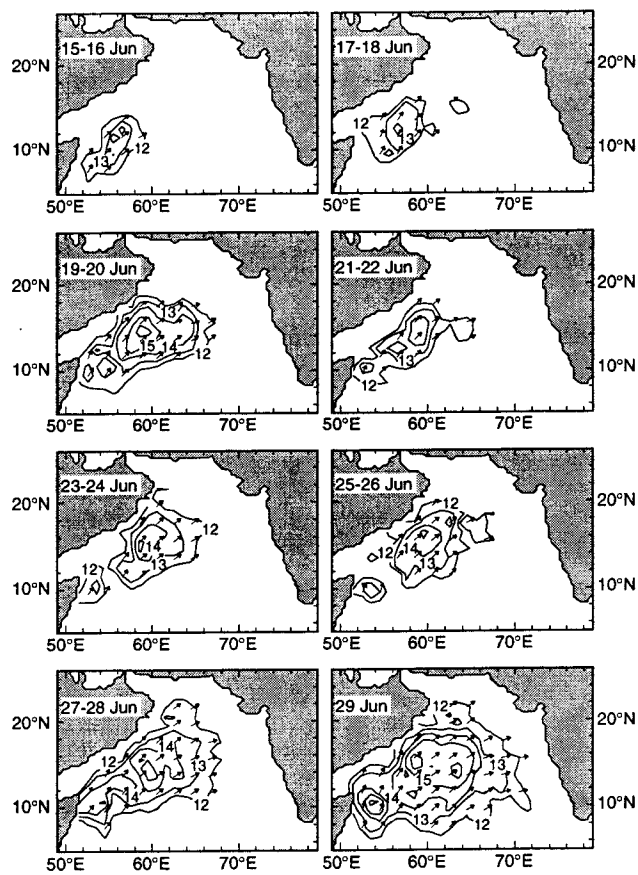


Figure 2



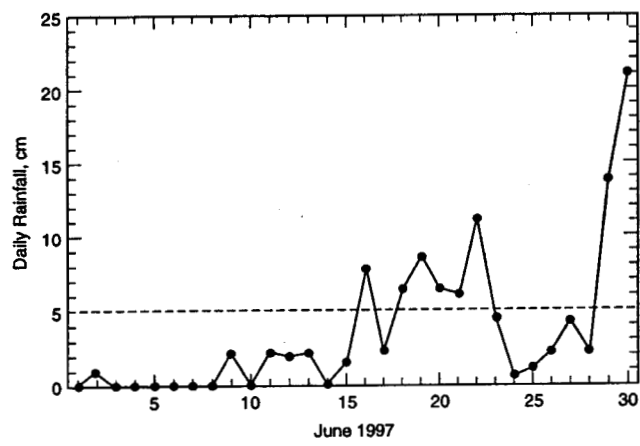


Figure 3

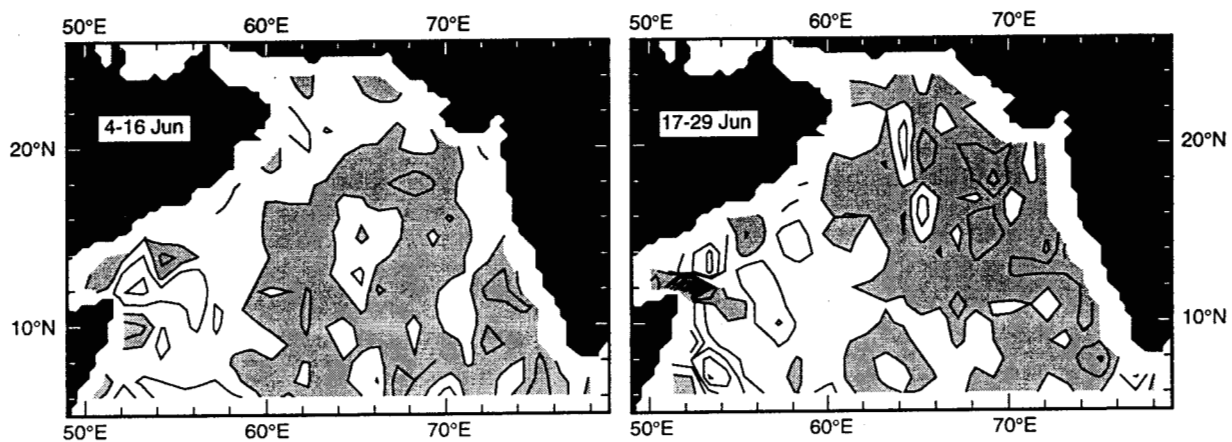


Figure 4

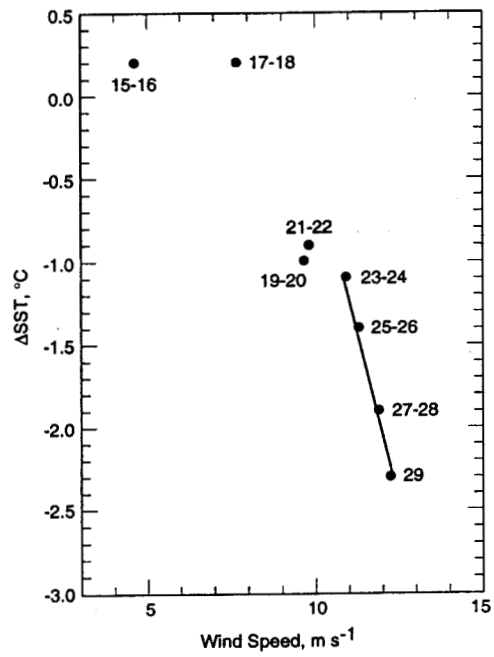


Figure 5

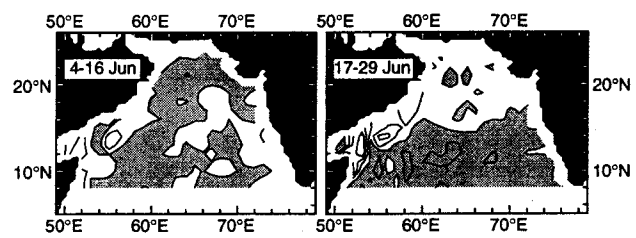


Figure 6